Effect of Ni on Amorphization of Ti-Cu-Ni Ternary Alloys Prepared by Mechanical Alloying

M. Ghadiri[a],*, A. Saidi[b]

[a] *Advanced Materials Research Center, Islamic Azad University, Najafabad Branch, Isfahan, Iran.*
[b] *Department of Materials Engineering, Isfahan University of Technology, Isfahan, Iran.*

ARTICLE INFO

ABSTRACT

Amorphous alloys have been taken into consideration because of their unique properties and are nominated as the future engineering materials. In this research, the effect of Ni and milling time on amorphization process and thermal stability of $Ti_{50}Cu_{50-x}Ni_x$ (x=10, 15, 25 at%) alloy system were investigated. The evolution of amorphization during mechanical alloying, thermal stability and subsequent heat treatment were evaluated by x-ray diffraction analysis (XRD) and differential scanning calorimetry (DSC). The results showed that alloys reached to the highest content of the amorphous phase in $Ti_{50}Cu_{40}Ni_{10}$, $Ti_{50}Cu_{15}Ni_{35}$ and $Ti_{50}Cu_{25}Ni_{25}$ alloy compounds after 60, 40, and 10 hours, respectively. Differential scanning calorimetry showed thermal stability of the amorphous alloy, exhibiting a distinct glass transition and crystallization temperature and a wide supercooled liquid region for $Ti_{50}Cu_{25}Ni_{25}$ powder alloy with a value about 45 k. Heating $Ti_{50}Cu_{25}Ni_{25}$ amorphous alloy at 943 K for 10 min results in the formation of intermetallics such as CuTi and $NiTi_2$ phases. In addition, mechanical properties of the amorphous powders were studied by Vickers microhardness test. The alloy with 25 percent Ni showed the high value of hardness about 884 H_v after 40 hours of mechanical alloying.

1. Introduction

The formation of the first metallic glass of $Au_{75}Si_{25}$ was reported by Duwez et al. at Caltech, USA, in 1960 [1]. They developed a technique in which a gaseous shock wave atomizes the molten metal into droplets (~ 10 mg) which are forced against a Cu chill block to form thin foils called splats. Through this splat quenching method, the molten metal can be subjected to cooling rates in excess of 10^5–10^6 K/s, thereby restricting the specimen geometry to thin ribbons, foils and powders, where at least one dimension was small enough, of the order of microns, to permit such a high cooling rate [1, 2].

Rapid solidification processing (RSP) [3] and solid state amorphization [4] are the most common ways for the synthesis of amorphous alloys. RSP has become an established route for the production of bulk amorphous alloys in

Corresponding author:
E-mail address: masoud_ghadiry@yahoo.com (Masoud Ghadiri).

the shape of thin ribbons, tubs, rods or amorphous matrix composites. Many methods for fabrication of bulk amorphous alloys by RSP such as centrifugal casting [5], water quenching [6], melt-spinning [7] and copper mold casting [8] have been developed. In recent years, solid state amorphization has gained considerable significance as an alternative route for synthesis of amorphous phases. The term solid state amorphization means that the amorphous phases are produced by solid state processing without involving melting and solidification stages [9]. The techniques of solid state amorphization include hydrogen-induced amorphization [10], diffusion annealing [11], cold rolling [12], mechanical alloying [13], and irradiation [14]. Among these techniques, mechanical alloying has become very popular because of its simplicity and the possibility of production of bulk shapes and sizes by suitable compaction techniques. There are basically two criteria used to select a binary alloy system for solid state amorphization. Firstly, the heat of mixing in the amorphous phase should be more negative than that of the crystalline solid solutions which provides the chemical driving force for solid state amorphization. Secondly, the diffusivity of one element into the other should be anomalously fast at the operating temperature. The second condition provides a kinetic constraint for the intermetallic compound formation, when the compound is more stable than the amorphous phase in these systems [15].

The notable feature of rapid solidification processing is that the glass-forming composition range is mainly restricted to deep eutectic regions due to kinetic constraints [1, 16].

Amorphization in Ti-Ni and Ti-Cu systems by mechanical alloying has been reported by many researchers. Amorphization in binary Ti-Ni system has been reported by Schwartz et al. [17] in the nickel content range 10-80 at.% Ni by mechanical alloying using a planetary ball mill. In another research, Schwartz and Petrich [18] reported amorphization in binary $Ti_{67}Ni_{33}$ composition by mechanical alloying using a Spex mill. Boldrick et al. [12] have reported a glass-forming composition range of Ni-(35-60)

at.% Ti in the Ni-Ti system by using a Spex mill. Amorphization in binary Ti-Ni system has been reported by Dobromyslov et al. [19] in the nickel content range 1-90 at.% Ni by mechanical alloying using a planetary ball mill.

Amorphization has been reported in many binary alloy systems by mechanical alloying, but reports on ternary alloy systems are very few. Ahn et al. [20] have investigated amorphization in Ti-Ni(50-x)-Cu(x) in the copper content range 5-20 at.% Cu by mechanical alloying without mentioning the kind of mill they used. Using a planetary ball mill, Murty et al. [9] have investigated amorphization in Ti-Ni, Ti-Cu binary and Ti-Ni-Cu ternary systems in the wet condition using a toluene medium to prevent oxidation of the powders. In the present study, amorphization in Ti-Cu-Ni ternary system in the titanium content 50 at.% Ti and nickel content range 10-25 at.% Ni has been investigated.

2. Experimental

The elemental powders of Ti, Cu and Ni (purity 99%; Merck Co. Germany) with the particle size of 90, 150 and 15 μm were mixed in proportions corresponding to the compositions of $Ti_{50}Cu_{50-x}Ni_x$(x=10, 15, 25 at%). The elemental blends were mechanically alloyed using an FP2 planetary ball mill with the speed of 300 rpm. Mechanical alloying was carried out in dry condition in hardened steel vials with ZrO_2 balls with 20 mm diameter, and the ball-to-powder weight ratio was kept at 20:1 during mechanical alloying. To avoid oxidation of the powder, the vials were evacuated and filled with Ar gas. To facilitate mechanical alloying process and to avoid adhesion of the powder to the inner wall of the vials, stearic acid was added as a PCA in a quantity of 1wt% of the total powder charge. The overall mechanical alloying time was 80 h and was interrupted every 60 min during the process. Each interruption lasted 15 min to cool down the vials. X-ray diffraction (XRD) using PHILIPS PW1800 diffractometer with Cu-Kα wavelength of 1.54059 A° was used for analysis of the phase formation in the milled powder samples. Thermal properties of the
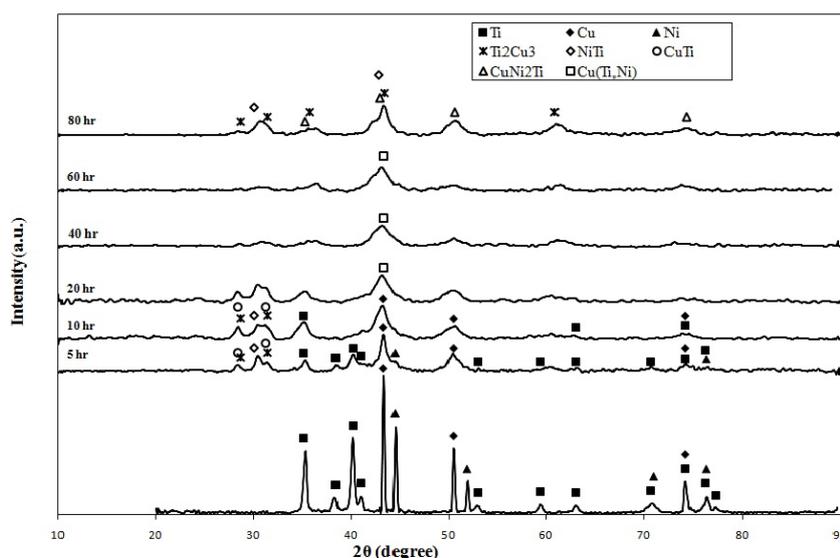
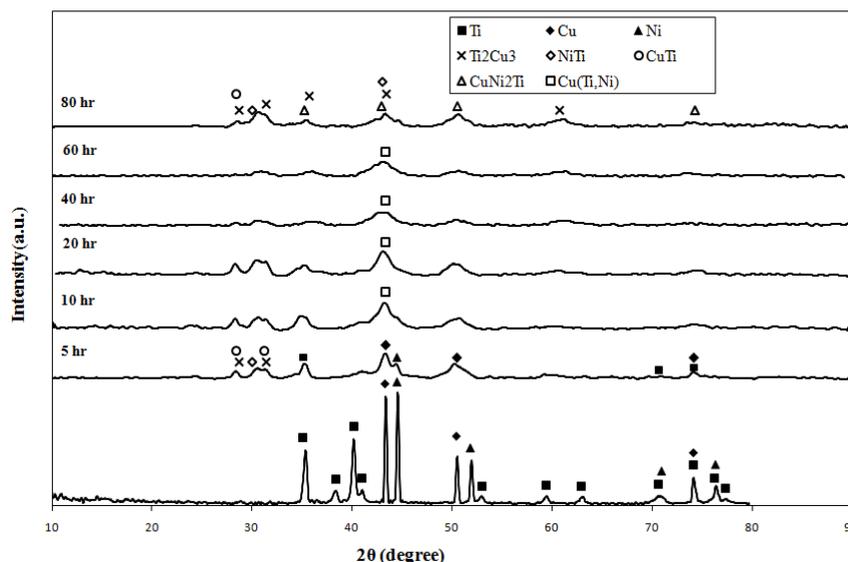**Fig. 1.** XRD patterns of the $Ti_{50}Cu_{40}Ni_{10}$ powder alloy after mechanical alloying for 5-80 h

as-milled amorphous powder were evaluated by SETARAM Labsys TG-DSC1600 and LINSEIS L81/1750 differential scanning calorimetry (DSC) with a heating rate of 20 K/min under a continuous flow of Ar gas. In addition, the Vickers microhardness of $Ti_{50}Cu_{25}Ni_{25}$ amorphous powder was measured under the ASTM E384 standard test method with a WOLPERT machine using a static load of 0.5 N.

3. Results and Discussion

Evolution of the amorphous phase during mechanical alloying process was monitored by means of XRD. The XRD patterns of $Ti_{50}Cu_{40}Ni_{10}$ powders after mechanical alloying times ranging from 0 to 80 h are shown in Fig 1. The bottom curve shows the XRD pattern of the unmilled powders. The most intense peaks corresponding to crystalline Ti, Cu and Ni elements are indexed in the pattern. A continuous decrease in intensity and broadening of the metal peaks are evident with increasing in mechanical alloying times as observed from 5-60 h. After mechanical alloying for 5 h, the intensity of the crystalline Ti and Cu peaks decreased and Ni peaks almost disappeared. After 10-40 h of mechanical alloying, decrease in intensity and broadening of the metal peaks are obvious from X-ray patterns and Ti peaks vanish completely. The intensity and broadening of crystalline peaks

are at the minimum and the maximum content after 60 h. Taking into consideration that atomic radii of Ni (0.125nm) and Cu (0.128nm) are approximately close to each other and the atomic radius of Ti (0.147 nm) is greater than Cu, shift of the Cu(111) peak to low angles and decrease in the intensity and broadening of the Cu and Ti peaks as well as disappearance of Ni peaks, is related to the formation of the Cu(Ni,Ti)-fcc solid solution that resulted in increasing the Cu lattice parameter with increase of mechanical alloying time to 60 h. After 80 h of mechanical alloying, the intensity of peaks slightly increased which showed recovery and crystallization of the powder because of increase in temperature during mechanical alloying, mechanical crystallization process and contamination of the milled powder. It seems that this alloy composition was not completely amorphized after 40 hours of mechanical alloying and showed low glass-forming ability (GFA) even after 80 h of processing.

Fig 2 shows the XRD patterns of the $Ti_{50}Cu_{35}Ni_{15}$ alloy powder after different mechanical alloying durations ranging from 0 to 80 hours. At the early stage of mechanical alloying (5 h), the crystalline Ti and Cu peaks were detected and Ni peaks almost vanished except for one peak at around 2θ=44.5°. The peak intensity of the crystalline Ti and Cu decreased significantly after 10 h of mechanical

Fig. 2. XRD patterns of the $Ti_{50}Cu_{35}Ni_{15}$ powder alloy after mechanical alloying for 5-80 h

alloying. In addition, all crystalline Ni peaks and some of Ti completely disappeared and considering that Cu peaks like Cu(111)-fcc shifted to low angles, this disappearance was related to the formation of Cu(Ni,Ti) solid solution that continue to 60 h. Traces of crystalline Cu with low intensity are still detected after mechanical alloying for 20 h but all crystalline Ti peaks vanish after this milling time. Traces of some crystalline Cu are still detected along with the amorphous phase after mechanical alloying for 40 h. No obvious differences in XRD patterns were observed even after mechanical alloying for 60 h, in comparison with the previous stage (40 h). The peaks intensity slightly increased after mechanical alloying for 80 h due to the temperature rising, mechanical crystallization and contamination of the milled powder during mechanical alloying process. Consequently, this alloy composition has the highest amorphous phase formation ability after mechanical alloying for 40 h and generally shows a relatively low GFA.

Similarly, the XRD patterns of the $Ti_{50}Cu_{25}Ni_{25}$ alloy powders are shown in Fig 3. The peak intensity of the crystalline Ti, Cu and Ni decreased significantly after 5 h of mechanical alloying. No change in the position of the crystalline Cu peaks was observed after this time, which indicates the solid solution formation. Significant changes in the intensity

and broadening of the peaks with continuing mechanical alloying for 10 hours were observed, and most of the crystalline Ti, Cu, and Ni peaks disappeared, which is related to formation of the Cu(Ni,Ti) solid solution as well as the new peaks in low angles due to formation of new phases after 10 hours of mechanical alloying. The shape of the XRD pattern after mechanical alloying for 10 h is similar to a smooth line that indicates the formation of the amorphous phase. In comparison with the previous duration, after 20 hours, the intensity of the peaks slightly increased that was due to recovery and crystallization of the previously formed amorphous phase and formation of the Cu(Ni,Ti) solid solution and increase in the lattice parameter of Cu that causes the shift of Cu peaks to low angles that is continued after 60 h of mechanical alloying (fig 4a). Similar to other alloy composition in this research, after mechanical alloying for 80 h the intensity of the peaks increased due to the temperature rising, mechanical crystallization, and contamination of the milled powder. Therefore, this alloy composition showed highest GFA in comparison with other alloys (figure1 and 2) and transformed to amorphous phases completely after mechanical alloying for 10 h. It was found that two conditions such as: (a) large negative heat of mixing in the amorphous phase and (b) anomalously fast diffusivity of
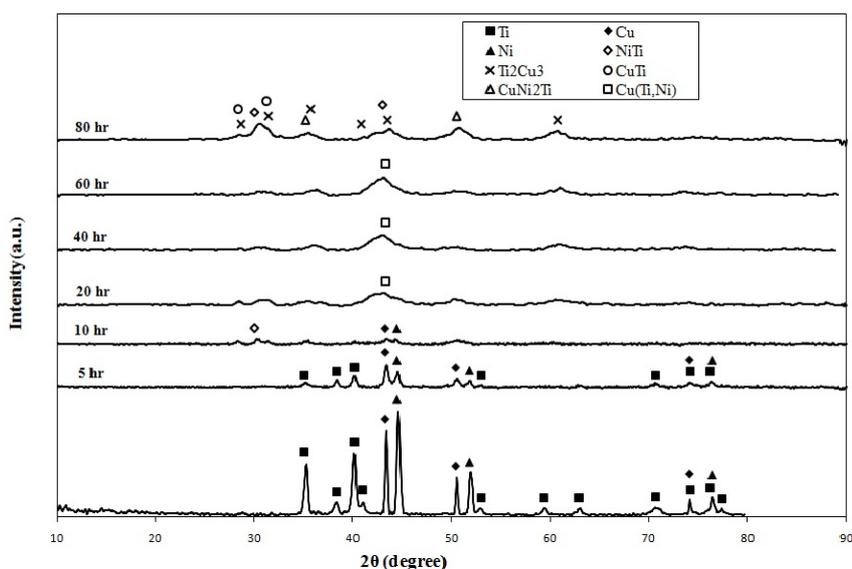
Fig. 3. XRD patterns of the $Ti_{50}Cu_{25}Ni_{25}$ powder alloy after mechanical alloying for 5-80 h
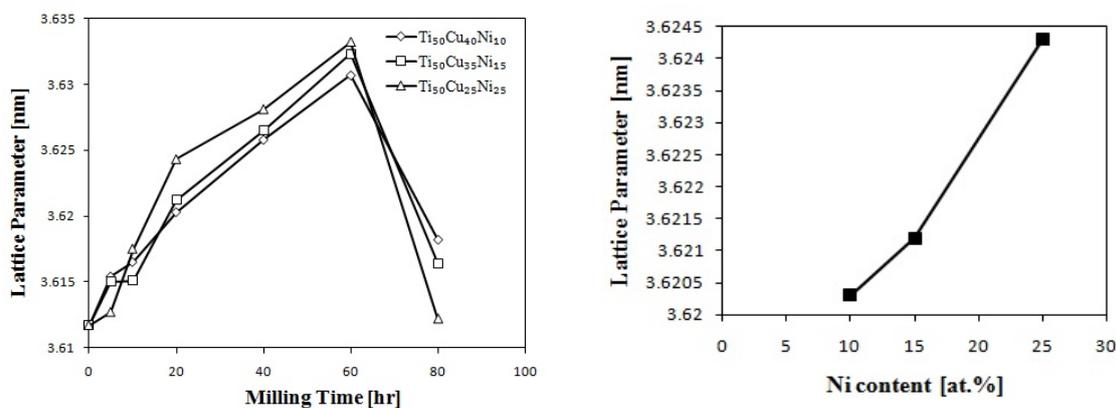

Fig. 4. (a) lattice parameter of the $Ti_{50}Cu_{40}Ni_{10}$, $Ti_{50}Cu_{35}Ni_{15}$ and $Ti_{50}Cu_{25}Ni_{25}$ compositions in the milled powder as a function of the milling time, (b) lattice parameter as a function of the Ni content after 20 h of mechanical alloying

one of the elements in the other, are necessary for a successful solid state amorphization reaction [17]. The heat of mixing between the Ni-Ti pairs is -35 kJ/mol, significantly larger than that of the Cu-Ti (-9 kJ/mol) pairs. Generally, the results showed that with increasing the Ni content the structure changes to amorphous phase in the earlier stages of mechanical alloying as observed in the case of $Ti_{50}Cu_{25}Ni_{25}$ alloy. It means that, the energy required for amorphization decreases with increasing the atomic percent of Ni element; therefore, Ni plays an important role in the GFA of Ti-based alloys. The present study has shown that the copper-rich alloys have lower

GFA in comparison with the alloys with higher content of Nickel. This is attributed to the higher energy required for amorohization. Similar results have been reported by Ahn et al. [20] in the case of $Ti_{50}Ni_{45}Cu_5$. It was also observed that the middle composition in the alloy composition, namely $Ti_{50}Cu_{25}Ni_{25}$, became amorphous within 10 h, indicating its faster rate of amorphization in comparison with other alloys. This shows that amorphization in dry condition (in the present study after 10 h) is faster than that in wet condition (Murty et al. [9] after 14 h) in the case of the $Ti_{50}Cu_{25}Ni_{25}$ alloy.

The mechanisms of solid-state amorphization
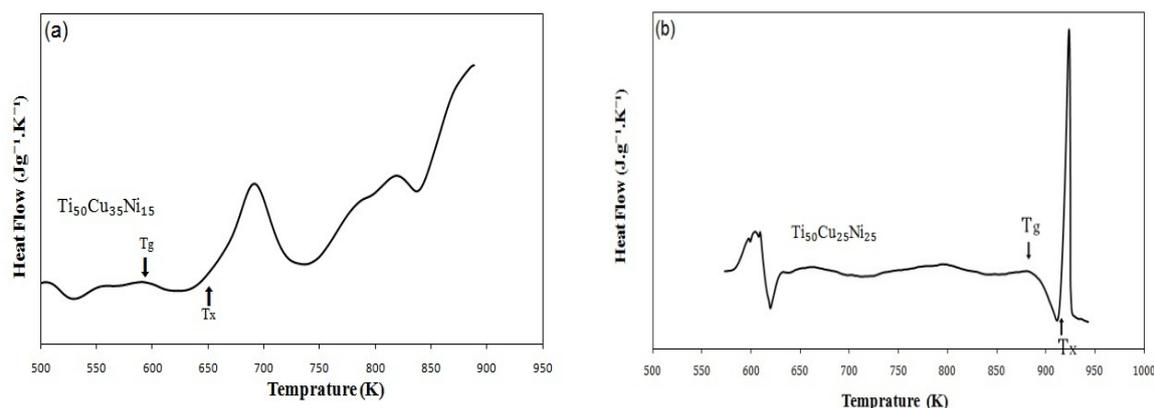
Fig. 5. DSC traces of the (a) $Ti_{50}Cu_{35}Ni_{15}$ and (b) $Ti_{50}Cu_{25}Ni_{25}$ amorphous powders after mechanical alloying for 40 and 10 h, respectively (heating rate of 20 K min^{-1})

Table 1. The glass transition (T_g), crystallization temperature (T_x) and SLR (ΔT_x) for $Ti_{50}Cu_{35}Ni_{15}$ and $Ti_{50}Cu_{25}Ni_{25}$ amorphous powders

Composition	Tg (k)	Tx (k)	ΔTx=Tx-Tg
$Ti_{50}Cu_{35}Ni_{15}$	596	638	42
$Ti_{50}Cu_{25}Ni_{25}$	877	922	45

in mechanically alloyed materials (in which intensive diffusion and plastic deformation take place) are associated with diffusion and/or plastic deformation. These amorphization mechanisms include the special, diffusion-induced migration of grain boundaries, the splitting of dislocations at three-way grain-boundary joints, and the formation of high-density ensembles of point defects [21]. Amorphization by mechanical alloying occurs as an increasing density of defects is introduced into the powder by heavy deformation until long range order crumbles by lattice instability. In the systems with largely negative heats of mixing and atom-size differences between components, the defects contribute most to the raising of the crystal lattice energy above amorphization that leads to stability of the amorphous phase [22, 23]. One of the most important mechanisms of amorphization is dissolution of some elements into the other element lattices that increases the elestic energy for the formation of the solid solution due to atomic size mismatch effect. This results in larger lattice parameter and leads to destabilization of the crystalline phase and formation of the amorphous phase [22]. In fig 4b, the changes in lattice parameter as a function of Ni content after 20 h of mechanical alloying are shown. It is obvious that by

increase in the Ni content from 10 to 25 at%, the lattice parameter of Cu increases continuously. It indicates that by increasing Ni, more contents of Ni dissolve into the Cu lattice and the lattice parameter increases more and this leads to destabilization of the Cu lattice and eventually the powder structure that favours the amorphization process.

Fig 5 shows the DSC traces of $Ti_{50}Cu_{25}Ni_{25}$ and $Ti_{50}Cu_{35}Ni_{15}$ after mechanical alloying for 10 and 40 h, respectively. The DSC curves exhibit an endothermic event characteristic of the glass transition, followed by a supercooled liquid region (SLR) $\Delta T_x=T_x-T_g$ and crystallization. The glass transition (T_g), crystallization temperature (T_x) and SLR (ΔT_x) are listed in table 1. The crystallization in the $Ti_{50}Cu_{25}Ni_{25}$ alloy proceeded in one stage, while it occurred in two stages in the $Ti_{50}Cu_{35}Ni_{15}$ alloy. It means that in the case of copper-rich elemental blends, where complete amorphization has not been observed even after mechanical alloying for 80 h, the crystallization peak is preceded by another exothermic peak. The SLR (ΔT_x) is a maximum at the midrange composition and the rate of amorphization is also the fastest for this composition.

The powders were heated in the DSC with a heating rate of 20 K/min at 943 k, held for 10
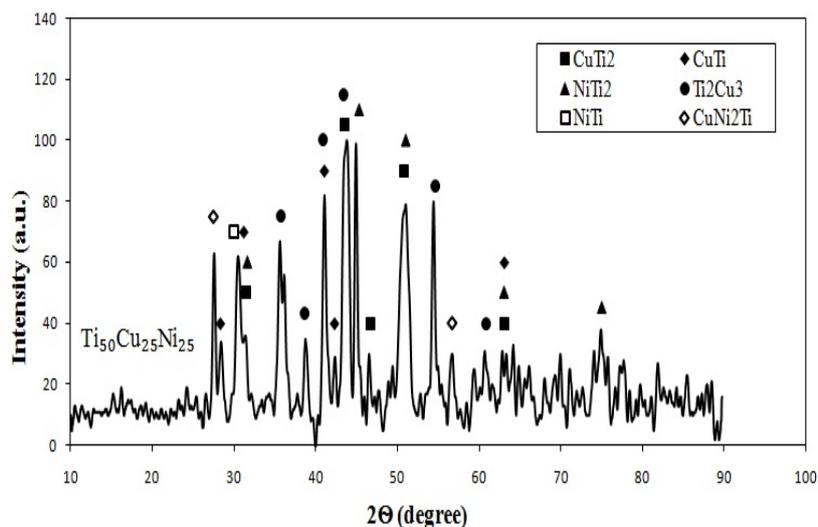
Fig. 6. The crystalline phases of the $Ti_{50}Cu_{25}Ni_{25}$ amorphous powder after heat treatment at 943 K for 10 min

Table 2. (a) Vickers microhardness of the $Ti_{50}Cu_{25}Ni_{25}$ amorphous powder as a function of the milling time, (b) average particle size as a function of milling time

composition	(a) Micro Hardness (Hv)			
	5 hr	10 hr	20 hr	40 hr
$Ti_{50}Cu_{25}Ni_{25}$	348	558	773	884
	(b) Average Particle Size (μm)			
	120	70	45	26

min and then cooled down to room temperature for the subsequent XRD measurements to identify the crystallization-relevant structural changes. Because amorphous alloys could be synthesized completely for $Ti_{50}Cu_{25}Ni_{25}$ composition after 10 h of mechanical alloying, this alloy composition was chosen as a model and investigated in detail. Heating of the $Ti_{50}Cu_{25}Ni_{25}$ amorphous alloy results in the formation of $CuNi_2Ti$, $NiTi_2$, $CuTi_2$, and Ti_2Cu_3 intermetallic phases as observed in Fig 6.

Results of the Vickers microhardness test and particle size of the mechanically alloyed powder are shown in Table 2. The hardness of the alloy powder increased by increasing milling time, so that after 10 h of mechanical alloying Vickers microhardness reaches to 558 H_v, which shows high value for the formed amorphous phase. By increasing mechanical alloying time some hard nanocrystalline phases are formed that are distributed in the amorphous matrix after 20 and 40 h of mechanical alloying and the hardness reaches

to the high value of 884 H_v. This value is comparable to the hardness of some Ni-based fully amorphous rectangular cast strips that has been reported by Xu et al. [24].

4. Conclusions

$Ti_{50}Cu_{50-x}Ni_x$(x=10, 15, 25 at%) alloys have been synthesized by mechanical alloying. The fully amorphous structure could be obtained in $Ti_{50}Cu_{25}Ni_{25}$ after 10 h of mechanical alloying. The $Ti_{50}Cu_{25}Ni_{25}$ alloy exhibited the highest thermal stability and amorphization ability and the largest supercooled liquid region of 45 K among alloys. The results of this study are promising for the development of the Ti–Cu–Ni amorphous alloys by powder metallurgy processing and the amorphous powder alloys with relatively large Supercooled Liquid Region ΔTx values (>40 K), which is beneficial for the consolidation of mechanically alloyed powders. Hardness Measurements of the $Ti_{50}Cu_{25}Ni_{25}$ alloy powder showed a considerable hardness value of 884 H_v after 40 h of mechanical alloying.

References

1. J. Basu, S. Ranganathan. "Bulk metallic glasses: A new class of engineering materials", Sadhana, Vol. 28, Parts 3 & 4, June/August 2003, pp. 783–798.

2. B. Ramakrishna Rao, "Bulk metallic glasses: Materials of future", DRDO Science Spectrum, March 2009, pp. 212-218.

3. H. Brequel, R. Badheka, F. Babonneau, and S. Enzo, "Study of amorphous compounds obtained by ball milling in the Si–C–O system", Journal of Materials Synthesis and Processing, Vol. 8, No. 5/6, 2000.

4. R. B. Schwarz, W. L. Johnson, "Remarks on solid state amorphizing transformations", Journal of the Less Common Metals, 1987.

5. R. Nowosielski, R. Babilas, "Fabrication of bulk metallic glasses by centrifugal casting method", Journal of Achievements in Materials and Manufacturing Engineering, Vol. 20, Issues 1-2, 2007.

6. J. Schroers, Y. Wu, R. Busch, W. L. Johnson, "Transition from nucleation controlled to growth controlled crystallization in $Pd_{43}Ni_{10}Cu_{27}P_{20}$ melts", Acta mater, 49, 2001, pp. 2773–2781.

7. J. Saida, H. Kato, A. Deny Heri Setyawan, A. Inoue, "Synthesis and properties of nanostructure controlled metallic glasses" Journal of Physics: Conference Series, 61, 2007, pp. 1002–1006.

8. W. Zhang, A. Inoue, "Formation and mechanical properties of Ni-based Ni–Nb–Ti–Hf bulk glassy alloys", Scripta Materialia, 48, 2003, pp. 641–645.

9. B. S. Murty, S. Ranganathan, M. Mohan Rao, "Solid state amorphization in binary Ti-Ni, Ti-Cu and ternary Ti-Ni-Cu system by mechanical alloying", Materials Science and Engineering A, Vol. 149, 1992, pp. 231-240.

10. T. Aihara, K. Aoki, T. Masumoto, "Formation and crystallization of hydrogen-induced amorphous RNi_2H_x (R=Sm, Gd, Dy, Ho, Er) alloys", Materials Transactions, JIM, Vol. 33, No. 1, 1992, pp. 15-22.

11. B. Blanpain, L. H. Allen, J. M. legresy, J. W. Mayer, "Solid-state amorphization in Al-Pt multilyers by low-temperature annealing", Physical Review B, vol. 39, No. 18, 1989, pp. 13067- 13071.

12. M. S. Boldrick, D. Lee, C. N. J. Wagner, "The Structure of amorphous Ni-Ti alloys prepared by mechanical alloying", Journal of Non-Crystalline Solids, 106, 1988, pp. 60-65.

13. C. Suryanarayana, E. Ivanovb, V.V. Boldyrev, "The science and technology of mechanical alloying", Materials Science and Engineering A, 304–306, 2001, pp. 151-158.

14. J. Koike, P. R. Okamoto, L. E. Rehn, M. Meshii, "The dose, temperature, and projectile-mass dependence for irradiation-induced amorphization of CuTi", Journal of Materials Research, Vol. 4, No. 5, 1989, pp. 1143-1150.

15. M. S. EL-Eskanarany, "Mechanical alloying for fabrication of advanced engineering materials", Noyes Publications United States of America, 2001.

16. J. Bhatt, B. S. Murty, "On the conditions for the synthesis of bulk metallic glasses by mechanical alloying", Journal of Alloys and Compounds, Vol. 459, 2008, pp. 135–141.

17. R. B. Schwarz, R. R. Petrich, C. K. Saw, "The synthesis of amorphous Ni-Ti alloy powders by mechanical alloying", Journal of Non-Crystalline Solids, Vol. 76, 1985, pp. 281-302.

18. R. B. Schwarz, R. R. Petrich, "Calorimetry study of the synthesis of amorphous Ni-Ti alloys by mechanical alloying", Journal of the Less-Common Metals, Vol. 140, 1988, pp. 171-184.

19. A. V. Dobromyslov, R. V. Churbaev, V. A. Elkin, T. L.Trenogina, "Mechanical alloying of Ti-Ni alloys under high pressure", Scripta Materialia., Vol. 41, No. 9, 1999, pp. 1015–1021.

20. I. S. Ahn, T. H. Nam, S. R. Bae, "Fabrication of mechanically alloyed TiNiCu powders and damping properties of Al/TiNiCu sintered materials", Metals and Materials, Vol. 3, No. 4, 1997, pp. 260-264.

21. I. A. Ovid'ko, A. V. Osipov, "Amorphization and shear microbands near grain boundaries in mechanically alloyed metallic materials", Tech. Phys, 42 (7), 1997, pp. 748-751.

22. C. Suryanarayana, "Mechanical alloying and milling", Progress in Materials Science, 46, 2001, pp. 1-184.

23. A. Reza Yavari, "Mechanically prepared nanocrystalline materials", Materials Transactions, JIM, Vol. 36, No 2, 1995, pp. 228-239.

24. D. Xu, G. Duan, W. L. Johnson, C. Garland, "Formation and properties of new Ni-based amorphous alloys with critical casting thickness up to 5 mm", Acta Materialia, 52, 2004, pp. 3493-3497